# The Role of $Mg^{2+}$ in the Inactivation of Inwardly Rectifying $K^+$ Channels in Aortic Endothelial Cells

TERYL R. ELAM* and JEFFRY B. LANSMAN‡

From the *Department of Physiology and ‡Department of Pharmacology, University of California School of Medicine, San Francisco, California 94143-0450

ABSTRACT We have studied the role of $Mg^{2+}$ in the inactivation of inwardly rectifying $K^+$ channels in vascular endothelial cells. Inactivation was largely eliminated in $Mg^{2+}$-free external solutions and the extent of inactivation was increased by raising $Mg_o^{2+}$. The dose-response relation for the reduction of channel open probability showed that $Mg_o^{2+}$ binds to a site ($K_D$ = ~25 μM at −160 mV) that senses ~38% of the potential drop from the external membrane surface. Analysis of the single-channel kinetics showed that $Mg^{2+}$ produced a class of long-lived closures that separated bursts of openings. Raising $Mg_o^{2+}$ reduced the burst duration, but less than expected for an open-channel blocking mechanism. The effects of $Mg_o^{2+}$ are antagonized by $K_o^+$ in manner which suggests that $K^+$ competes with $Mg^{2+}$ for the inactivation site. $Mg_o^{2+}$ also reduced the amplitude of the single-channel current at millimolar concentrations by a rapid block of the open channel. A mechanism is proposed in which $Mg^{2+}$ binds to the closed channel during hyperpolarization and prevents it from opening until it is occupied by $K^+$.

## INTRODUCTION

There is now abundant evidence which indicates that $Mg^{2+}$ prevents the flow of outward current through the inwardly rectifying $K^+$ channels of cardiac and skeletal muscle by blocking the channel pore during depolarization (Vandenberg, 1987; Matsuda, Saigusa, and Irisawa, 1987; Matsuda, 1988; Burton and Hutter, 1989; Ishihara, Mitsuiye, Noma, and Takano, 1989). There is less information concerning the mechanism which causes the inward current through the channels to decline during hyperpolarization (Ohmori, 1978; Standen and Stanfield, 1979; Sakmann and Trube, 1984*b*; Matsuda and Stanfield, 1989; Harvey and Ten Eick, 1989; Silver and DeCoursey, 1990). Evidence suggests that the decay of inward current results from block of the channel by extracellular $Na^+$ (Ohmori, 1978; Fukushima, 1982). Sakmann and Trube (1984*b*), however, observed inactivation of the inward current in the absence of extracellular $Na^+$ and concluded that inactivation was due either to block of the channel pore by divalent cations at physiological concentrations or to an

Address correspondence to Dr. Jeffry B. Lansman, Department of Pharmacology, School of Medicine, University of California, San Francisco, CA 94143-0450.

J. GEN. PHYSIOL. © The Rockefeller University Press · 0022-1295/95/04/0463/22 $2.00
Volume 105 April 1995 463–484

intrinsic gating process. Biermans, Vareecke, and Carmeliet (1987) showed that removing divalent cations from the external solution reduced the extent of inactivation, suggesting a blocking mechanism. The blocking mechanism, however, has not been tested at the single-channel level.

The experiments in this paper investigated the role of $Mg^{2+}$ in the gating of single inwardly rectifying $K^+$ channels in aortic endothelial cells. The results show that $Mg^{2+}$ inhibits both the inward and outward currents through the channel. Block of the outward current is sufficiently fast that it is likely to account for the rapid rectifying properties of this channel. Inactivation of the inward current cannot be explained by a simple model in which $Mg^{2+}$ blocks the open channel. The results suggest, instead, that inactivation arises from the binding of $Mg^{2+}$ to the closed channel. $K^+$ competes with $Mg^{2+}$ for occupancy of this site in a manner suggesting close coupling between $K^+$ transport and channel opening. Preliminary results of this work have been reported as abstracts (Elam and Lansman, 1990, 1992).

## METHODS

### *Preparation of Cells*

Bovine aortas were obtained from local slaughterhouses (Hoehner Meat Packing Co., San Leandro, CA; Ferrera Meats, San Jose, CA). The descending aorta was isolated and rinsed with a cold $Ca^{2+}$-free saline solution containing 5 U/ml of heparin. The vessel was stored in a cold HEPES buffered Dulbecco's Modified Eagle Medium (DMEM) containing streptomycin and penicillin for transport back to the laboratory.

Endothelial cells were isolated after the procedure described by Pearson, Slakey, and Gordon (1983). Excess connective tissue was removed from the exterior of the aorta and the distal end and accessory vessels were sutured shut. The vessel was filled with a warm (37°C) solution of 0.2% collagenase B (Boehringer Mannheim Corp., Indianapolis, IN) in DMEM, clamped shut and incubated at 37°C for ~15 min. The perfusate and one rinse with DMEM were collected and centrifuged at 100 *g* for 4 min. The cell pellet was washed twice with DMEM, resuspended in a growth media consisting of DMEM containing 20% fetal calf serum, 5% glutamine, and antibiotics, and plated into 35-mm tissue culture dishes (Corning Glass, Inc., Corning, NY). Cultures were maintained at 37°C in an atmosphere of 5% $CO_2$/95% air. The tissue culture media was replaced every 1–2 d with fresh media. Endothelial cells were identified by their characteristic cobblestone morphology when grown to confluence and by immunofluorescent staining for Von Willebrand's Factor (Jaffe, Nachman, Becker, and Minick, 1973). Cultures were used for experiments during the first five passages when they had reached ~50–75% confluency. We found during the course of these experiments that the density of inwardly rectifying $K^+$ channels changed with time in culture. Freshly dissociated cells had a low density of channels which increased with time (data not shown). During the first few days in culture, only about a third of the recordings from cell-attached patches contained channel activity. By day 14 (fourth passage), membrane patches often contained five or more channels.

### *Electrophysiological Methods*

Single-channel activity was recorded from cell-attached and cell-free membrane patches following the technique described by Hamill, Marty, Sakmann, Sigworth, and Neher (1981). Patch electrodes were made from Boralex hematocrit glass (Rochester Scientific, Rochester, NY) and had resistances of 3–7 MΩ with 150 mM KCl in the patch electrode and 150 mM K-aspartate in the bath. Membrane seal resistances ranged from 5–30 GΩ.

The bathing solution was an isotonic K-aspartate solution which contained 150 mM aspartic acid, 150 mM KOH, 2 mM $MgCl_2$, 10 mM glucose, 1 mM EGTA, and 10 mM HEPES. A $Mg^{2+}$-free K-aspartate solution was made by omitting $Mg^{2+}$ and adding 10 mM EDTA and 2 mM EGTA. The isotonic $K^+$ bathing solution was used to zero the cell membrane potential so that the patch potential would be the same as the voltage command applied to the patch clamp amplifier. In some experiments, the single-channel current-voltage relation was measured after excising the patch from the cell surface. The shift of the single-channel current-voltage relation indicated a maximum voltage error of ~10 mV.

The electrode filling solution contained 150 mM KCl, 2 mM $MgCl_2$, 10 mM glucose, and 10 mM HEPES. In experiments in which the $Mg^{2+}$ concentration of the external solution was varied, $Mg^{2+}$ and EDTA were added at appropriate concentrations according to the equations given by Blinks, Wier, Hess, and Prendergast (1982) to give the final free $Mg^{2+}$ concentration. The concentration of $K^+$ was varied by replacing it with an equimolar concentration of choline chloride. The osmolarity of the solutions was adjusted to 290–310 mosm by adding glucose. The pH was adjusted to 7.4 by adding KOH. All experiments were done at room temperature (22–24°C).

### *Data Analysis*

Current signals were recorded with a List-EPC-7 amplifier and stored on video tape (A. R. Vetter Co., Inc., Rebersburg, PA). In some experiments, currents were recorded directly onto the hard disk of the computer . Current signals were filtered with an eight-pole Bessel filter (−3 dB) and digitized at 0.05–2.0 ms directly onto the hard disk of a laboratory computer (LSI 11/73) for analysis.

Open- and closed-time durations were measured from idealized records produced by a half-threshold detection method (Colquhoun and Sigworth, 1983). Histograms of open- and closed-time durations were fit with the sum of up to three exponential components by use of a maximum-likelihood fitting routine. The fits to the histograms of open and closed times were corrected for missed events by setting a cutoff at 0.4 ms which was subtracted from the maximum-likelihood estimate of the time constants. Channel open probability ($P_o$) was calculated by dividing the total length of the current record by the sum of the idealized open times measured from the single-channel currents.

Bursts of channel activity were defined as a series of rapid transitions between the open and closed states that were separated by longer-lived $Mg^{2+}$-dependent closures (see Fig. 8). The duration of the $Mg^{2+}$-dependent closures was measured by fitting the sum of three exponentials to the histograms of all closed times. The interburst interval was assumed to be equal to the time constant of the slowest component. Burst lengths were measured by excluding all closures in the record that were shorter than a set cut-off value. We chose 300 ms as the cut-off time because it is at least four times the mean duration of the longest $Mg^{2+}$-independent closures. This cut-off ensures that fewer than ~2% of the $Mg^{2+}$-independent closures will be mistakenly counted as $Mg^{2+}$-dependent closures. This method of defining a burst, however, overestimates the true burst lifetime because it misses all $Mg^{2+}$-dependent closures less than the cut-off value. The true burst durations were calculated from the measured burst durations following the procedure described by Blatz and Magleby (1986):

$$t_{b(true)} = t_{b(app)} * \exp(-t_c/t_{ibi}) - t_{ibi}[1 - (1 + t_c/t_{ibi}) \exp(-t_c/t_{ibi})], \quad (1)$$

where $t_{b(true)}$ is the true burst duration, $t_{b(app)}$ is the measured apparent burst duration, $t_c$ is the cut-off time (300 ms), and $t_{ibi}$ is the duration of the $Mg^{2+}$-dependent interburst intervals.

## RESULTS

Previous studies have shown that vascular endothelial cells express inwardly rectifying $K^+$ channels (Johns, Freay, Adams, Lategan, Ryan, and VanBreemen, 1987; Takeda, Schini, and Stoeckel, 1987; Olesen, Clapman, and Davies, 1988; Silver and Decoursey, 1990). Silver and DeCoursey (1990) studied whole-cell inward rectifier currents in vascular endothelial cells and concluded that virtually all the rectification is independent of intracellular $Mg^{2+}$ ($Mg_i^{2+}$). We reexamined the role of $Mg_i^{2+}$ in the mechanism of inward rectification at the single-channel level to determine whether the channels in endothelial cells differ from those in cardiac and skeletal muscle.

Fig. 1 shows the single-channel activity recorded from a cell-attached patch at different holding potentials. The patch electrode contained 150 mM KCl and 2 mM $Mg^{2+}$. The single-channel current-voltage relationship was linear with a slope conductance of 24.1 ± 2.9 pS (mean ± SD, $n$ = 13) in 150 mM KCl. This value is similar to that reported for inwardly rectifying $K^+$ channels in other cells (ventricular myocytes: Sakmann and Trube, 1984*a*; macrophages: McKinney and Gallin, 1988;

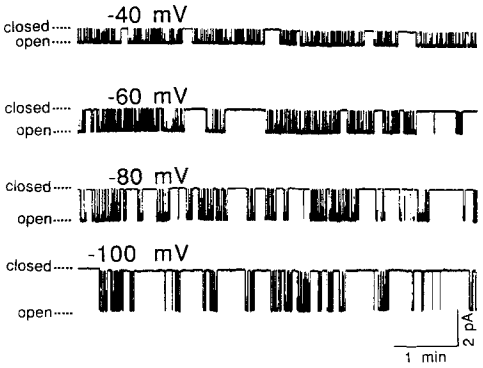


FIGURE 1. Single-channel currents recorded from a cell-attached patch which contained a single inwardly rectifying $K^+$ channel. The patch electrode contained 150 mM KCl sand 2 mM $MgCl_2$. Each record represents ~6 min of continuous channel activity at the indicated holding potential. Currents were sampled at 500 Hz and filtered at 100 Hz.

skeletal muscle: Matsuda and Stanfield, 1989). Consistent with the behavior of inwardly rectifying $K^+$ channels, the reversal potential shifted ~59 mV for a 10-fold change in $K_o^+$ and the single-channel conductance varied with the square root of $K_o^+$ (Hagiwara and Takahashi, 1974).

### *$Mg^{2+}$ Block of Outward Current through the Channel*

Analysis of the role of $Mg_i^{2+}$ in blocking the outward current through these channels is hampered by the rundown of activity in excised membrane patches. Fig. 2 *A* shows an experiment in which a patch was excised into a bathing solution which contained millimolar $Mg^{2+}$. Channel activity persisted for only ~20 s after excision of the patch from the cell surface (*arrowhead*). We found, however, that prior addition of 0.5 mM 8-bromo-cyclic-adenyl-monophosphate (8-Br-cAMP) to the bath slowed the loss of channel activity after patch excision. Fig. 2 *B* shows an experiment in which 0.5 mM 8-Br-cAMP was added to the bathing solution at the start of the experiment. In this experiment, channel activity remained high after excision. In the cells pretreated with 8-Br-cAMP, channel activity persisted for 16.0 ± 9.6 min (mean ± SEM, $n$=5).

8-Br-cAMP did not appear to act directly on the channel because adding it to the bath after the channel activity dissappeared did not restore it to previous levels (data not shown). Fig. 2 *C* shows, on the other hand, that there was virtually no loss of channel activity when patches were excised into a $Mg^{2+}$-free bathing solution. In this experiment, channel activity persisted for more than 20 min. These results show that $Mg^{2+}$ at the cytoplasmic surface causes a relatively rapid rundown of channel activity, perhaps by promoting channel dephosphorylation. In the experiments described

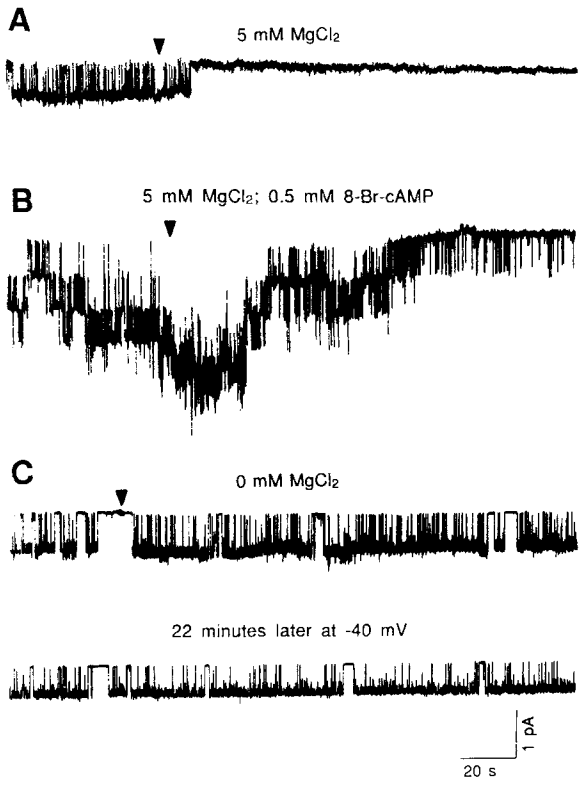


FIGURE 2. Effects of internal $Mg^{2+}$ on the stability of channel activity in membrane patches. (*A*) Single-channel currents recorded from a cell-attached patch before and after excision of the patch into a solution containing 150 mM K-aspartate and 5 mM $MgCl_2$. The arrow indicates the time at which the patch was excised from the membrane. (*B*) Single-channel currents recorded from a different patch before and after excision into a solution containing 150 mM K-aspartate and 5 mM $MgCl_2$ to which 0.5 mM 8-Br-cAMP was added. There were about four channels in this patch. (*C*) Single-channel currents recorded from a patch before and after excision into an $Mg^{2+}$-free, 150 mM K-aspartate solution. Each record represents ~3.5 min of continuous channel activity recorded at a holding potential of −50 mV in *A* and *B* and −60 mV in *C*. Currents were filtered at 100 Hz and sampled at 500 Hz.

below, patches were excised directly into a $Mg^{2+}$-free bathing solution to minimize rundown.

Fig. 3 *A* provides evidence that $Mg_i^{2+}$ blocks the flow of outward current through the channel. Although there were clearly resolved inward currents when the patch was held at −40 mV, there was no detectable single-channel activity at +40 mV. After excising the patch into the $Mg^{2+}$-free bathing solution, both inward and outward currents were detected (Fig. 3 *B*). The single-channel current-voltage relationship

before and after excision into the $Mg^{2+}$-free bathing solution was linear (Fig. 3 *C*). After patch excision, the single-channel conductance was 22.6 ± 1.3 pS and current reversed at +3.3 ± 4.9 mV (mean ± SD, $n$=3), similar to the values obtained in recordings from cell-attached patches. It was unlikely that the $Mg_i^{2+}$-free solution unmasked silent channels, because outward currents were detected after excision only when inward currents were initially present and the number of channels in the patch did not change.

Although removing $Mg_i^{2+}$ produced outward currents, channels opened only transiently during the positive voltage step. Fig. 4 *A* shows the outward currents in the $Mg^{2+}$-free bath solution during a long voltage step. The voltage step to +50 mV

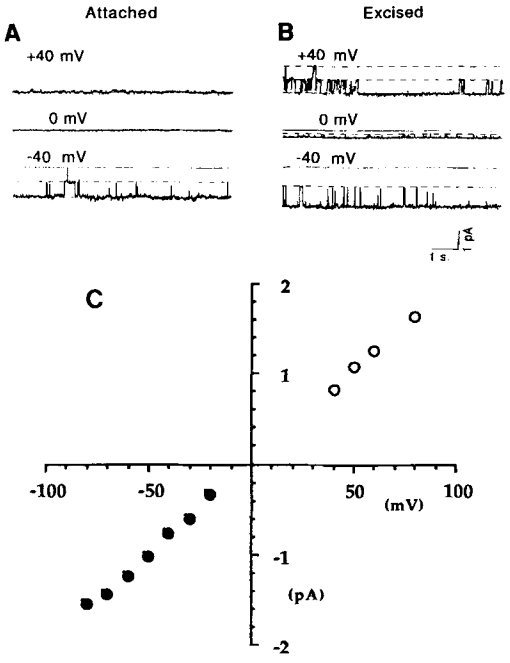


FIGURE 3. Outward currents produced by the removal of internal $Mg^{2+}$. (*A*) Single-channel currents recorded from a cell-attached patch which contained two channels. There were no outward currents when the patch was held at +40 mV. (*B*) Single-channel currents recorded after excising the patch into a $Mg^{2+}$-free (< 1 nM) K-aspartate solution showing the outward currents flowing through the channel at +40 mV. In this experiment, there was a voltage offset of ~10 mV when the patch was excised into the $Mg^{2+}$-free solution. The electrode contained a $Mg^{2+}$-free, KCl solution. Currents were sampled at 1 kHz and filtered at 200 Hz in both *A* and *B*. (*C*) The amplitude of single-channel currents recorded from an excised membrane patch plotted as a function of the patch holding potential. The current-voltage relationship was linear and reversed near zero mV. The conductance was 22.6 pS (mean ± SD, $n$ = 3).

produced an initial burst of openings at the onset of the pulse. After the initial burst of openings, however, the channel remained closed and reopened only infrequently. The time course of the $Mg_i^{2+}$-independent gating of the outward current was measured by holding the patch potential at −40 mV and then stepping it to positive test potentials. The currents recorded in response to repetitive voltage steps were averaged to obtain the mean current at each test potential. Fig. 4 *B* shows the mean currents recorded from a single patch in response to voltage steps to +40, +60, +80, and +100 mV. Fig. 4 *C* shows the time constants describing the decay of the mean currents that were obtained by fitting the records with a single exponential. At potentials more positive than ~ +70 mV, the rate of decay became essentially voltage

insensitive. The results are consistent with the idea that $Mg_i^{2+}$ produces a rapid block of outward current, but that there is an intrinsic voltage-dependent gating process that causes channel closure in the absence of $Mg_i^{2+}$ (Matusda, 1991).

*$Mg^{2+}$-dependent Inactivation of Inward Current*

Fig. 5 shows the inactivation of the inwardly rectifying $K^+$ channels during membrane hyperpolarization (see also Sakmann and Trube, 1984*b*). In these experiments, the

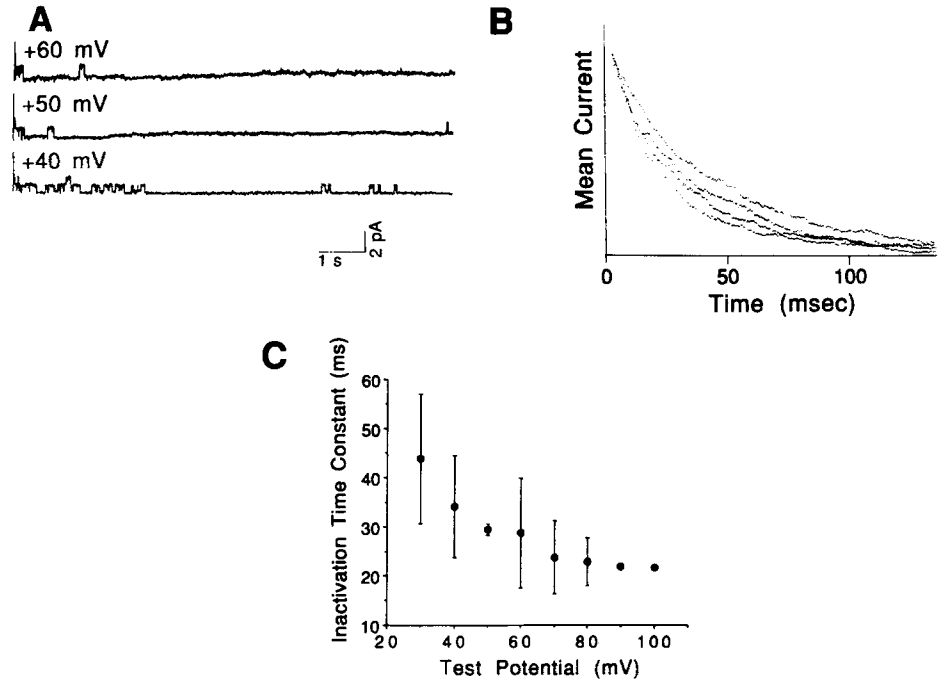


FIGURE 4. Time course of the outward current through inwardly rectifying $K^+$ channels in the absence of internal $Mg^{2+}$. (*A*) Outward currents recorded in response to a voltage step from a holding potential of −40 mV to the indicated test potentials. Recording from a membrane patch excised into a $Mg^{2+}$-free internal solution. Current records were filtered at 1 KHz and sampled at 5 KHz. (*B*) Voltage dependence of the outward current.The mean currents were obtained from averaging the outwards currents that were evoked in response to ~90 identical voltage steps to either +40, +60, +80, and +100 mV (from top to bottom). (*C*) The time constant of the single exponential fit to the decay of the outward current was plotted as a function of the potential of the test pulse (mean ± SD, $n$=4).

single-channel activity was measured from patches containing one to five channels. During hyperpolarizing voltage steps, the single-channel activity was high at the beginning of the test pulse and then decreased (Fig. 5 *A*). The mean current at each test potential was obtained by averaging the individual current responses to a large number of identical test pulses. Fig. 5 *B* shows the mean currents obtained in one such experiment scaled so that the peak amplitudes are the same. The decay of the

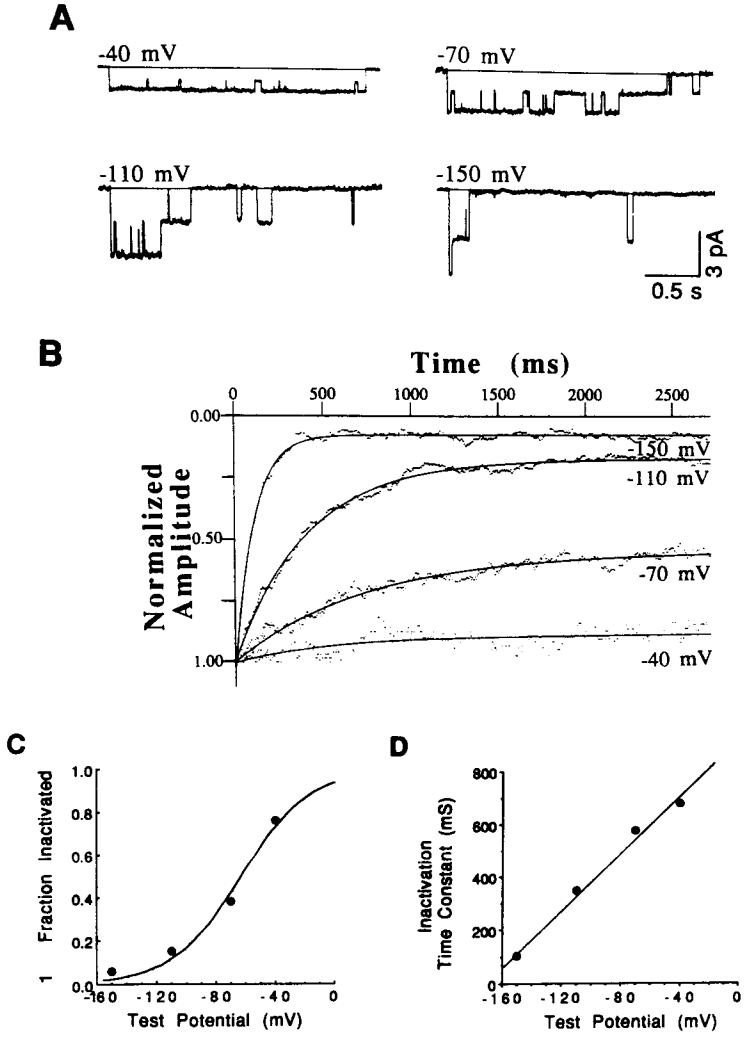


FIGURE 5. Voltage-dependent inactivation of the inward current during hyperpolarizing voltage steps. (*A*) Single-channel currents recorded during voltage steps to −40, −70, −110, or −150 mV from a holding potential of 0 mV that lasted 2,720 ms. The solid lines indicate zero-current levels in each record. Leak and capacitive currents were subtracted. The patch electrode contained 150 mM KCl and 2 mM $MgCl_2$. Currents were sampled at 1 KHz and filtered at 200 Hz. (*B*) Time course of the mean current at different test potentials. Mean currents were obtained by averaging the current responses to 70–100 identical voltage steps to the indicated potentials. The smooth lines through the currents are the fits to a single exponential decaying to a nonzero level. The mean currents are normalized so that initial amplitudes are the same. (*C*) Dependence of the extent of inactivation of the mean current on the test pulse potential. Fraction of channels remaining open at the end of the voltage step was obtained from the amplitude of the steady state current divided by the amplitude of the current at $t=0$. The points are fit to a Boltzmann distribution with half inactivation of −63 mV and slope of 23 mV. (*D*)Dependence of the rate of inactivation of the mean current on the test pulse potential. The time constants for the decay of the mean current was obtained from the single-exponential fit and plotted as a function of the test pulse potential.

mean current was well fit by a single exponential function decaying to a nonzero level (*solid lines*). Both the extent of inactivation (Fig. 5 *C*) and its rate (Fig. 5 *D*) depended on membrane potential.

We examined the effect of extracellular $Mg^{2+}$ ($Mg_o^{2+}$) on the voltage-dependent

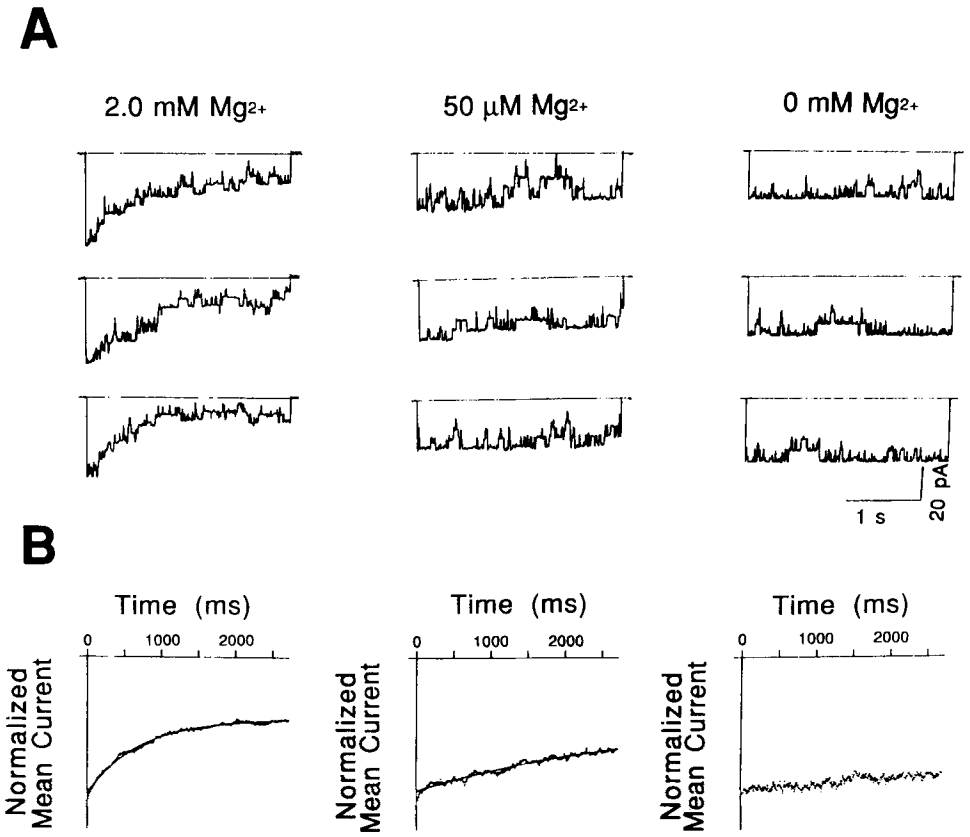


FIGURE 6. Effect of external $Mg^{2+}$ on time course of inactivation. (*A*) Single-channel activity recorded from cell-attached patches in which the patch electrode contained either 2 mM, 50 μM, or 0 $Mg_o^{2+}$. Patches contained approximately five to seven channels. The patch was held at 0 mV then stepped to −120 mV for 2,720 ms. (*B*) The mean currents obtained by averaging the current responses to ~100 identical voltage steps to −120 mV from 0 mV with either 2 mM, 50 μM or 0 mM $Mg^{2+}$ in the patch electrode. The mean currents were fit by single exponentials decaying to a nonzero level. In the presence of 2 mM $Mg_o^{2+}$, the current decayed to 46% of its initial value by 695 ms, with 50 μM $Mg_o^{2+}$, the current decayed to 72% of its initial by 2,074 ms. Records were corrected for leak and capacitive currents.

inactivation of the inward current. Recordings were made from multichannel patches exposed to different concentrations of $Mg_o^{2+}$. The patch potential was held at 0 mV and then stepped to different test potentials for ~3 s before returning to the holding potential. Fig. 6*A* shows that with 2 mM $Mg^{2+}$ in the electrode, single-channel

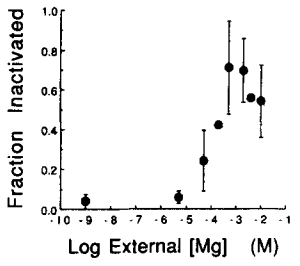


FIGURE 7. The effect of external $Mg^{2+}$ concentration on the extent of inactivation. Mean currents were fit by a single exponential. The extent of inactivation was determined in each experiment as the steady state current during the voltage step to −120 mV divided by the current at $t$=0. Each data point is the mean ± SD ($n$=2–5). $Mg_o^{2+}$ produced half-maximal inactivation at ~300 μM.

activity decayed rapidly. In the absence of $Mg_o^{2+}$, the inward current showed little inactivation. Inactivation depended only on the presence of $Mg_o^{2+}$, because excising a patch into bathing solutions containing either zero (< 1 nM) or 2 mM $Mg^{2+}$ had no effect on the inactivation time course in either the presence of absence of $Mg_o^{2+}$ in the patch electrode (data not shown).

Fig. 7 shows that increasing $Mg_o^{2+}$ increased the extent of inactivation, with half-maximal inactivation at $Mg_o^{2+}$ = ~300 μM. At millimolar concentrations, however, inactivation was incomplete and was even reduced at concentrations exceeding several millimolar. Although the extent of inactivation depended on $Mg_o^{2+}$, the rate of inactivation did not change systematically with $Mg_o^{2+}$ over a three orders of magnitude concentration change (data not shown). If $Mg^{2+}$ acts by occluding the channel pore, then the rate as well as the extent of inactivation is expected to depend on $Mg_o^{2+}$ (e.g., Armstrong, 1969). That the rate was relatively insensitive to $Mg_o^{2+}$ indicates that the mechanism is likely to be more complicated than occlusion of the open channel. This issue is considered in more detail below.

Fig. 8 shows that $Mg_o^{2+}$ causes the gating of the single channel to occur in well-defined bursts of openings (Sakmann and Trube, 1984*b*). In the absence of

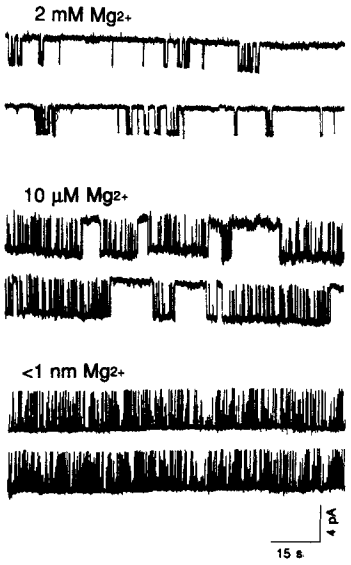


FIGURE 8. Single-channel activity in the presence of different concentrations of $Mg_o^{2+}$. The patch electrode contained 150 mM KCl solutions and either 2.0 mM, 10 μM, or 0 (< 1 nM) $Mg^{2+}$. The membrane potential was held at −120 mV. Currents were sampled at 500 Hz and filtered at 100 Hz.

$Mg_o^{2+}$, the channel fluctuated rapidly between open and closed states, but was open ~95% of the time. By contrast, channel activity recorded in the presence of either 2 mM or 10 μM $Mg_o^{2+}$ occured in bursts that were separated by long closed periods. In addition to its effects on gating, $Mg_o^{2+}$ reduced the amplitude of the single-channel current at millimolar concentrations. Shioya, Matsuda, and Noma (1993) reported that high concentrations of $Mg^{2+}$ produced a rapid block of inwardly rectifying $K^+$ channels in ventricular myocytes. The results shown in Fig. 9 support the idea that

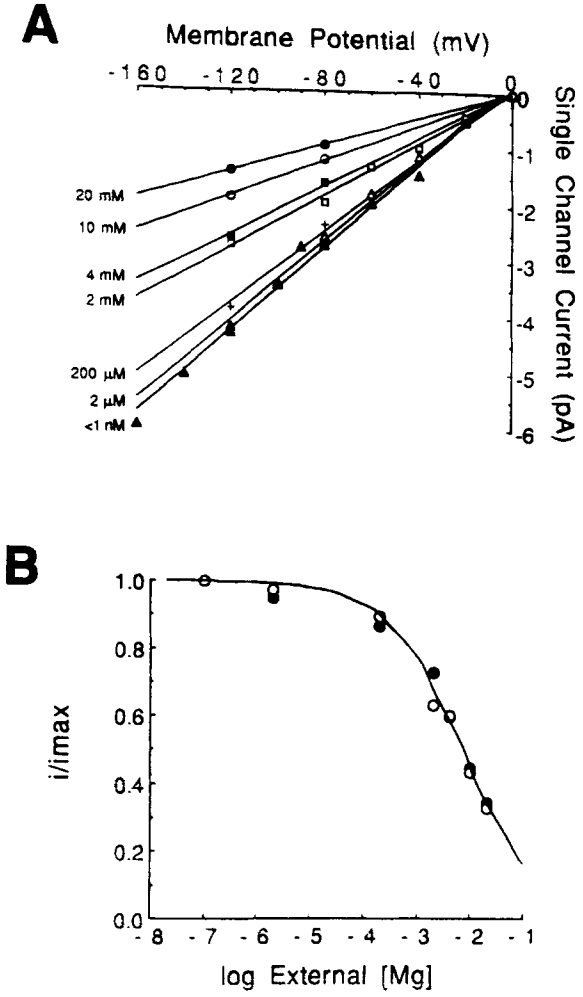


FIGURE 9. Reduction of the amplitude of the single-channel current by $Mg_o^{2+}$. (*A*) Single-channel current-voltage relationships measured in the presence of various concentrations of $Mg_o^{2+}$. The single-channel conductances were 37, 35, 32, 23, 21, 16, and 12 pS awith $Mg_o^{2+}$ = <1 nm, 2 μM, 200 μM, 2, 4, 10, and 20 mM, respectively. (*B*) Fractional reduction of the single-channel current ($i/i_{max}$) with increasing $Mg_o^{2+}$ at two different membrane potentials (*open circles*, −120 mV; *filled circles*, −80 mV). The apparent $K_D$ = ~8 mM at both −120 and −80 mV. Each data point represents the mean of two to seven recordings. The patch electrode contained 150 mM KCl with the indicated concentration of $Mg^{2+}$.

$Mg^{2+}$ reduces the single-channel current by binding to a low affinity site. Fig. 9 *A* shows the single-channel current-voltage relation as a function of $Mg_o^{2+}$. The amplitude of the single-channel current was reduced when $Mg_o^{2+}$ exceeded ~200 μM. Fig. 9 *B* shows the reduction of the single-channel current with increasing $Mg_o^{2+}$ at −120 mV (*open circles*) and −80 mV (*filled circles*). The apparent $K_D$ was ~8

mM and independent of membrane potential. The value of the $K_D$ for the fast blocking process is similar to that reported by Shioya et al. (1993).

Evidently, there is a low affinity $Mg^{2+}$ blocking site located outside the membrane field ($K_D$ = 8 mM), as well as a higher affinity site ($K_D$ = ~300 μM) associated with the inactivation process. We analyzed the dose-response relationship to determine the location of the high affinity inactivation site within the membrane field. If the $Mg^{2+}$ binding site lies within the membrane field, then the apparent affinity is expected to depend on membrane potential according to the model of Woodhull (1973). Fig. 10 shows that the relationship between channel open probability and

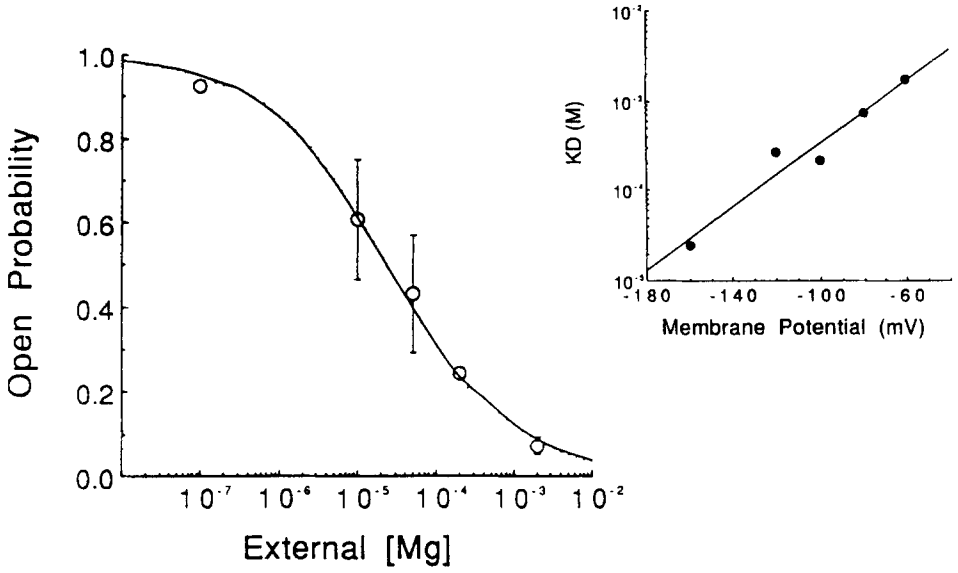


FIGURE 10. Dose-response relation for the reduction of channel open probability by $Mg_o^{2+}$. Each point represents the mean ± SEM. The data were fit by Eq. 4 with a Hill coefficient of 0.48 and $K_D$ = 25 μM. The Hill coefficient was unaffected by the membrane potential over the entire range examined. (*Inset*) Change in the apparent binding affinity ($K_D$) with membrane potential. The $K_D$ decreased ~10-fold/33 mV hyperpolarization.

$Mg_o^{2+}$ can be fit with a relationship of the form:

$$P_o = P_{max} - P_{max}\{[^n/(1 + (K_D/Mg^{2+})^n]\} \quad (2)$$

where $P_o$ is the channel open probability in the presence of $Mg^{2+}$ (at −160 mV), $P_{max}$ is the maximum open probability in the absence of $Mg_o^{2+}$, $K_D$ is the apparent dissociation constant, and $n$ is the Hill coefficient describing the steepness of the change in open probability with $Mg_o^{2+}$. The fit to the experimental points gave a $K_D$ = ~25 μM at −160 mV and a Hill coefficient ($n$) of 0.54 ± 0.03 (mean ± SEM, $n$ = 5). Fig. 10 (*inset*) shows that the $K_D$ depended strongly on membrane potential. The dependence of the apparent $Mg^{2+}$ affinity on membrane potential was fit to a relation describing a voltage dependent binding equilibrium of the form:

$$K_D(V) = K_D(0) \exp(-z\partial VF/RT) \quad (3)$$

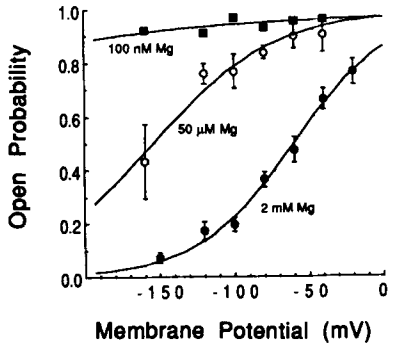


FIGURE 11. The effect of membrane potential on channel open probability (mean ± SEM) in the presence 100 nM ($n$ = 3–9), 50 μM ($n$ = 2–7), or 2 mM external $Mg^{2+}$ ($n$ = 7–13). The solid lines represent the fit to a Boltzmann relations with steepnesses ($k_v$) of 41 mV and 32 mV/$e$-fold and half-activation potentials ($V_{1/2}$) of −154 and −60 mV in 50 μM, and 2 mM external $Mg^{2+}$, respectively.

where z is the valence of the blocking particle and $d$ is the fractional electrical distance between the external surface of the membrane and the $Mg^{2+}$ binding site (Woodhull, 1973). The slope of the regression line gave a value of $d$ = 0.38 ± 0.07, (mean ± SEM), suggesting that $Mg^{2+}$ binds to a site that is located ~38% of the potential drop from the external membrane surface.

The results of Fig. 10 are replotted in Fig. 11 to show the voltage-dependent gating in the presence of different $Mg_o^{2+}$. With $Mg_o^{2+}$ reduced to ~100 nM, there was only a small change in opening probability with voltage over the range studied. With $Mg_o^{2+}$ equal to 50 μM or 2 mM, the relationship between channel open probability and voltage was well fit by a Boltzmann relation. The relation measured with $Mg_o^{2+}$ = 2 mM was shifted along the voltage axis towards positive potentials by ~100 mV compared with that measured in the presence of 50 μM $Mg_o^{2+}$. There was also a corresponding increase in the steepness of the relation (~$e$-fold per 32 and 41 mV in 2 mM and 50 μM $Mg_o^{2+}$, respectively). The magnitude of the shift is much larger than

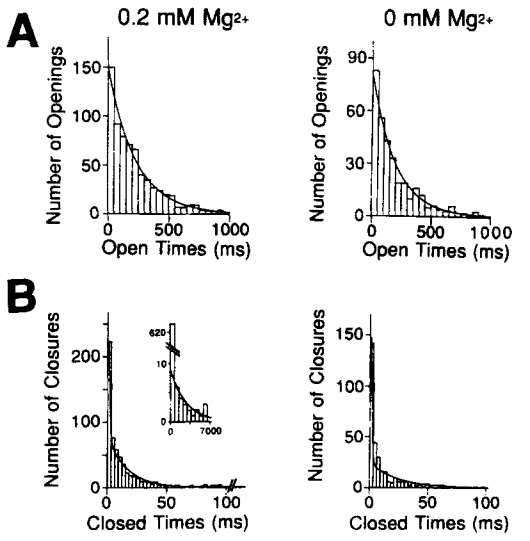


FIGURE 12. Effect of $Mg_o^{2+}$ on channel opening and closing rates. (*A*) Histograms of open times in either the presence or absence of $Mg^{2+}$ were well fit by single exponentials with similar time constants. In the presence of external 0.2 mM $Mg^{2+}$, $t_o$ = 228 ms whereas in the absence of external $Mg^{2+}$, $t_o$ = 200 ms. (*B*) Histograms of closed times in the presence of $Mg_o^{2+}$ were fit by three exponential components. In the absence of $Mg_o^{2+}$, only two exponentials were required to fit closed time distribution. (*Inset*) Histogram of long-lived closures (>250 ms) which are observed when $Mg^{2+}$ is present in the electrode solution. The time constants and relative amplitudes of the multiexponential fit to the closed time distribution are 0.84 ms (.29), 17.3 ms (.61), and 2,803 ms (.10) in the presence of 0.2 mM external $Mg^{2+}$ and 0.72 ms (.44) and 24.5 ms (.56) ms in in the absence of $Mg_o^{2+}$. The patch potential was −80 mV.

expected for a reduction of the membrane surface potential by $Mg_o^{2+}$ (e.g., Ohmori and Yoshii, 1977).

Subsequent experiments investigated the effects of $Mg_o^{2+}$ on the single-channel kinetics. Fig. 12 *A* shows the histograms of channel open times that were obtained from measurements of channel activity in the presence or the absence of $Mg_o^{2+}$. The open time histograms were well fit by a single exponential, consistent with the existence of a single open state. Fig. 12 *B* shows that at least three exponential components were required to fit the histogram of channel closed times in the presence of $Mg^{2+}$. In the absence of $Mg^{2+}$, however, only two components were required to fit the distribution of closed times. The kinetic constants obtained from

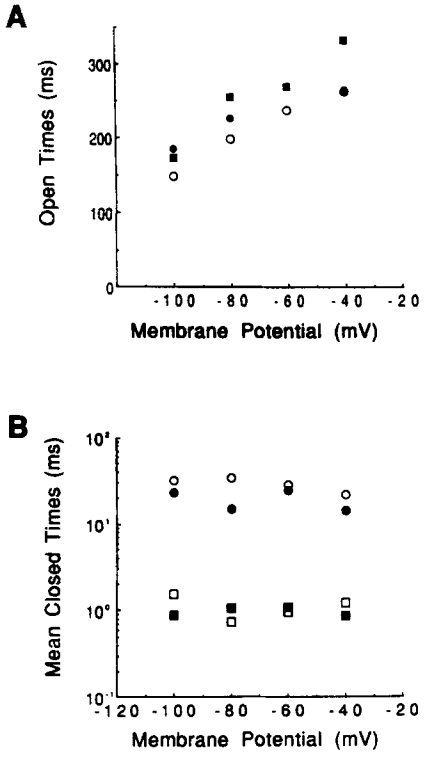


FIGURE 13. The voltage dependence of channel opening and closing is not affected by $Mg_o^{2+}$. (*A*) The mean open time plotted as a function of membrane potential (*filled squares*, 2 mM $Mg_o^{2+}$; *filled circles*, 0.2 mM $Mg_o^{2+}$; *open circles*, 0 $Mg_o^{2+}$). (*B*) Time constants of the two rapid components of the closed time distribution plotted as a function of membrane potential (*filled symbols*, 0.2 mM $Mg_o^{2+}$; *open symbols*, 0 $Mg_o^{2+}$).

from the exponential fits to the open and closed time distributions are shown in Fig. 13. Fig. 13 *A* shows that as the holding potential was made more positive, the mean open time increased, both in the presence (*filled symbols*) or absence (*open symbols*) of $Mg_o^{2+}$. There was a small prolongation of the mean open time in the presence of $Mg_o^{2+}$ which may arise from a reduction in the closing rate when the fast block site is occupied. Fig. 13 *B* shows that durations of the two brief closed periods were also relatively insensitive to external $Mg_o^{2+}$. The results shown in Figs. 12 and 13 indicate that $Mg_o^{2+}$ produces slow closures in the single-channel records, but does not affect channel opening and closing within a burst.

Previous studies have suggested that the inactivation of inwardly rectifying $K^+$

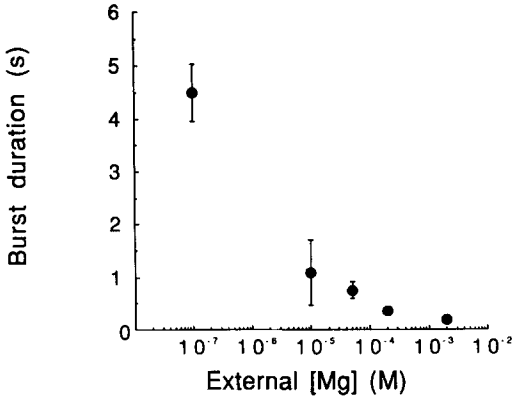


FIGURE 14. Dependence of the burst duration on $Mg_o^{2+}$. Measurements from channel activity recorded at −120 mV (mean ± SEM, $n$=3–11).

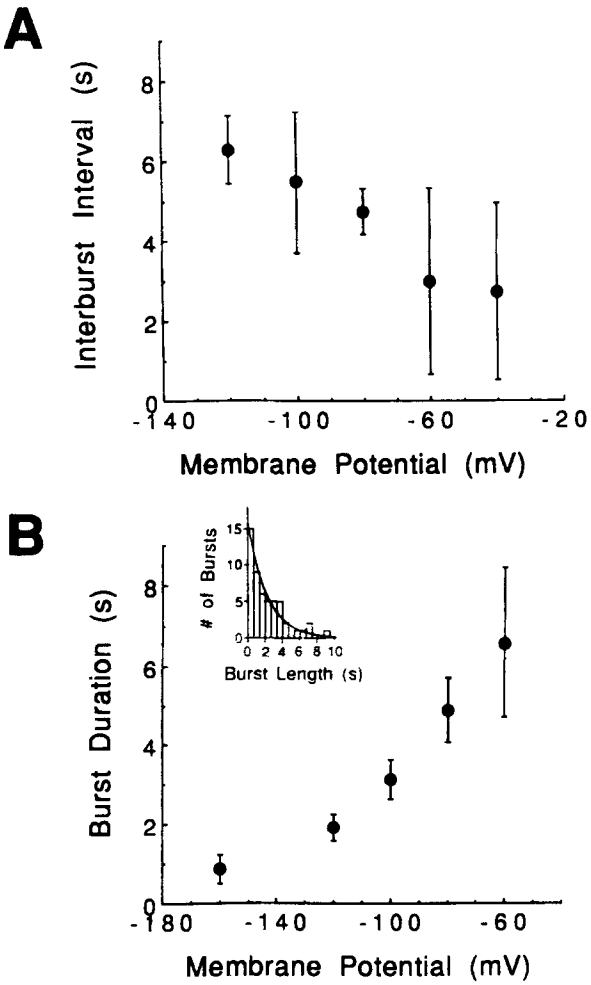


FIGURE 15. Voltage dependence of the burst kinetics in the presence of 2.0 mM $Mg_o^{2+}$. (*A*) The interburst interval plotted as a function of membrane potential. (*B*) The burst duration plotted as a function of membrane potential. (*Inset*) The distribution of burst durations showing that it is well fit by a single exponential. Each data point represents the mean ± SEM for two to seven patches.

channels involves block of the open channel by a physiological ion (Fukushima, 1982; Sakmann and Trube, 1984*b*; Biermans et al., 1987). The effects of $Mg^{2+}$ on the single-channel current are strikingly reminiscent of pore-blocking behavior in which the slow transitions between bursts and intervening silent periods reflect $Mg^{2+}$ entry and exit from the pore. The predictions of an open-channel blocking mechanism, however, have not been rigorously tested. The $Mg_o^{2+}$-dependent gating transitions (bursts and interburst intervals) are much slower than $Mg_o^{2+}$-independent opening

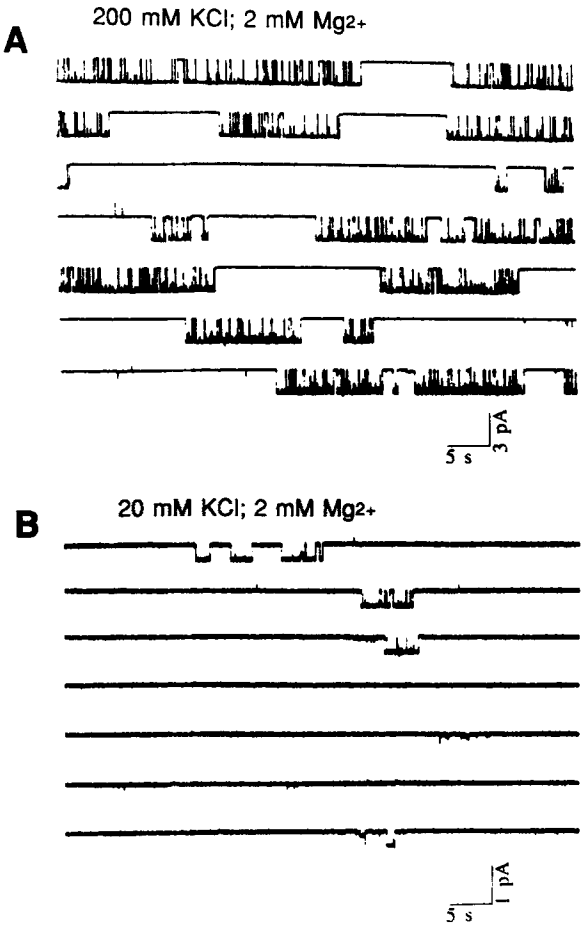


FIGURE 16. The effect of $K_o^+$ on the single-channel activity in the presence of 2 mM $Mg_o^{2+}$. (*A*) Single-channel activity recorded from a cell-attached patch. The patch electrode contained 200 mM KCl and 2 mM $Mg^{2+}$. (*B*) Single-channel activity recorded from another cell-attached patch. The electrode contained 20 mM KCl and 2 mM $Mg^{2+}$. Each record represents ~7 min of continuous channel activity at −80 mV. Channel open probability was 0.54 in 200 mM KCl and 2 mM $Mg^{2+}$ and 0.04 in 20 mM KCl and 2 mM $Mg^{2+}$. Currents were sampled at 500 Hz and filtered at 100 Hz.

and closing transitions. Consequently, the slower transitions between the $Mg^{2+}$-dependent bursts and interburst intervals can be used to obtain the apparent rates of $Mg^{2+}$ association and dissociation from its site.

If $Mg^{2+}$ binds to the open channel, then the reaction follows bimolecular kinetics and the inverse of the burst duration is linearly related to $Mg_o^{2+}$. Interburst intervals represent the first-order dissociation of $Mg^{2+}$ from its binding site and are concentration independent. Burst durations and interburst intervals were measured as

described in the Methods. Fig. 14 shows the effect of $Mg_o^{2+}$ on the burst duration. We found that a ~100-fold change in $Mg_o^{2+}$ reduced the burst duration only fourfold, considerably less than expected for a bimolecular reaction between $Mg^{2+}$ and the open channel. The slow bursting kinetics in the presence of $Mg_o^{2+}$ are, nonetheless, consistent with the movement of the postively charged cation to a binding site within the membrane field. Fig. 15 *A* shows that hyperpolarization prolonged the interburst interval, as expected if $Mg^{2+}$ is held more tighlty at its binding site by the imposed voltage. Hyperpolarization also reduced the burst duration in a manner consistent with an enhanced entry rate for a positively charged molecule.

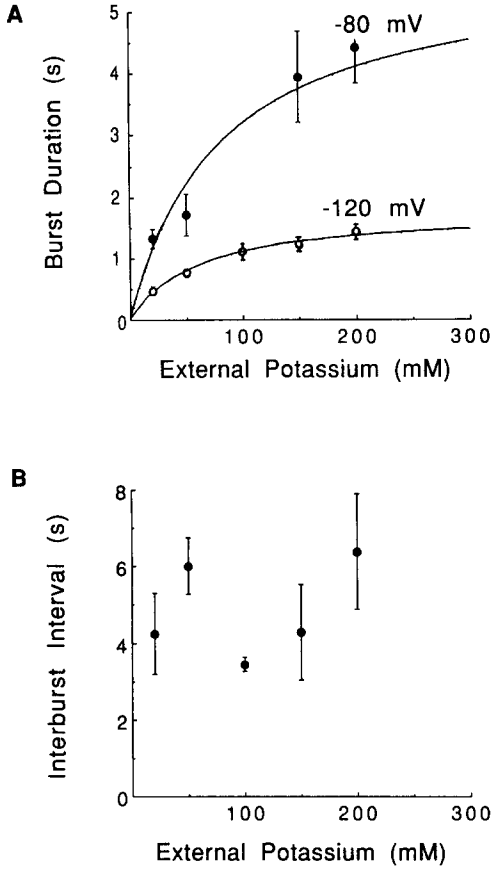


FIGURE 17. Effect of $K_o^+$ on the $Mg^{2+}$-dependent bursts and interburst intervals. (*A*) Burst durations plotted as a function of $K_o^+$ (mean ± SE, $n$=3–7; *filled circles*, holding potential = −80 mV; *open circles*, holding potential = −120 mV). The apparent $K_D$ was ~90 mM at −80 mV and ~60 mM at −120 mV. (*B*) Mean lifetime of the $Mg^{2+}$-dependent closures plotted as a function of $K_o^+$ (mean ± SEM, $n$=3–7).

*Effect of External $K^+$ Concentration*

The voltage dependence of the $Mg_o^{2+}$-dependent bursts and interburst intervals provides additional support for a binding site that is located within the membrane field. In the subsequent experiments, we asked whether the permeant ion $K^+$ can also bind to this site. Fig. 16 shows the single-channel activity in the presence of 200 mM $K_o^+$ (*top record*) and in the presence of 20 mM $K_o^+$ (*bottom record*). The duration of the

bursts and of the $Mg^{2+}$-dependent interburst intervals were measured in the presence of different concentrations of $K_o^+$, but with $Mg_o^{2+}$ fixed at 2 mM. In high $K_o^+$ (200 mM), the burst duration is longer than in the presence of low $K^+$ (20 mM). Fig. 17 *A* shows that, at a fixed $Mg^{2+}$ concentration, the burst duration increased as $K_o^+$ was increased and could be fit with a simple saturating function for one to one binding. The apparent $K_D$ for $K^+$ was ~90 mM at −80 mV (*filled symbols*) and 120 mM at −120 mV (*open symbols*). Fig. 17 *B* shows that, by contrast, the $Mg^{2+}$-dependent interburst intervals did not depend on $K_o^+$. The prolongation of the burst duration can be explained if $K^+$ competes with $Mg^{2+}$ for a site in the channel.

## DISCUSSION

The results in this paper show that inward rectification in bovine aortic endothelial cells arises from $Mg^{2+}$-dependent and -independent gating processes. The $Mg^{2+}$-dependent rectification is fast (Sakmann and Trube, 1984*b*), while the $Mg^{2+}$-independent rectification is much slower and is voltage dependent. While both of these components may contribute to the inward rectification in vascular endothelial cells, the high concentration of $Mg_i^{2+}$ and rapid time course of the $Mg^{2+}$-dependent suppression of outward current suggests that, under physiological conditions, $Mg_i^{2+}$ is likely to contribute substantially to the inward rectification of the $K^+$ channels in endothelial cells.

### *Voltage-dependent Inactivation*

During hyperpolarization, the current through inwardly rectifying $K^+$ channels inactivates. The effects of $Mg_o^{2+}$ on the inactivation process can be summarized as follows. (*a*) Removing $Mg_o^{2+}$ largely eliminates inactivation. (*b*) $Mg_o^{2+}$ reduces channel open probability at negative voltages more than at more positive voltages. (*c*) $Mg_o^{2+}$ produces a class of long-lived closures, but does not affect the rapid transitions between the closed and open states within a burst. (*d*) $Mg_o^{2+}$ reduces the duration of the bursts of openings, but less than expected for a bimolecular reaction with the open channel. The last observation and the finding that the rate of inactivation did not depend on $Mg_o^{2+}$ made it necessary to reject a simple open channel blocking mechanism. Thus, the mechanism of $Mg^{2+}$-dependent inactivation of inwardly rectifying $K^+$ channels differs from the inactivation of delayed $K^+$ currents produced by quatenary ammonium compounds (Armstrong, 1969).

The voltage dependence of the inactivation process was consistent with a simple model in which $Mg^{2+}$ binds to a site within the membrane field. A similar conclusion was reached by Fukushima (1982) who studied the inactivation of single inwardly rectifying $K^+$ channels by $Sr^{2+}$ in a tunicate egg cell. The electrical distance for the inactivation site was estimated at 34% of the potential drop from the external surface (Fukushima, 1982), close to the value of 38% found for $Mg^{2+}$ in this study. Unlike the inactivation produced by $Sr^{2+}$, however, we found no evidence for relief of inhibition at large negative membrane potentials. Consequently, $Mg^{2+}$ does not appear to exit towards the cytoplasmic surface once it has bound. This conclusion is further supported by the finding that exposing the cytoplasmic surface to high $Mg_i^{2+}$ in the absence of $Mg_o^{2+}$ did not cause inactivation.

The effects of $K_o^+$ on the burst kinetics suggested that $K^+$ competes with $Mg^{2+}$ for a single site. We found no evidence for an effect of $K_o^+$ on the interburst interval that would suggest ion–ion interactions in multiple binding sites. The apparent $K^+$ affinity that was estimated from the prolongation of the burst duration by $K_o^+$ was voltage dependent. This finding suggests that $K^+$ binding is also influenced by the applied voltage. In addition, the affinity of $K^+$ for the inactivation site was similar to the affinity measured from the dependence of the single-channel conductance on $K_o^+$. Thus, $Mg^{2+}$ may bind to a site that is normally occupied by $K^+$ during ion transport.

It is possible to account for many of the experimental observations by a model in which $Mg^{2+}$ binds to the channel only when it is in the closed state

$$\mathrm{CB}_{1(\mathrm{Mg})} \overset{\text{slow}}{\langle\text{-}\rangle} C \overset{\text{fast}}{\langle\text{-}\rangle} O \tag{4}$$

where $C$ represents the $Mg_o^{2+}$-independent closed states, $O$ is the open state, and $CB_1$ is the $Mg^{2+}$-bound closed state (the two $Mg^{2+}$-independent closed states have been lumped together). The equations relating the rate constants in the model to the experimentally measured burst durations and interburst intervals are given in Sakmann and Trube (1984*b*, their Eqs. 10 and 19). It is noted here that the inverse of the interburst interval is approximately equal to the $Mg^{2+}$ dissociation rate, because $Mg^{2+}$ association is slow compared with opening. Because there are two $Mg^{2+}$ binding sites that can be reached from the outside, however, Eq. 4 must be modified to account for the rapid block of the open channel

$$\mathrm{CB}_{1(\mathrm{Mg})} \overset{\text{slow}}{\langle\text{-}\rangle} C \overset{\text{fast}}{\langle\text{-}\rangle} O \overset{\text{fast}}{\langle\text{-}\rangle} \mathrm{OB}_{2(\mathrm{Mg})} \tag{5}$$

where $OB_2$ has been added and is the open-blocked state ($d$=0). If the channel cannot close easily when $Mg^{2+}$ occupies the fast block site, then the probability that $Mg^{2+}$ will bind to the closed channel is reduced. One prediction of the model that is born out by the results is that inactivation is incomplete and is even reduced as the fast block site becomes occupied a larger fraction of the time at high $Mg_o^{2+}$. Moreover, the finding that the dose-response relation is less steep than expected for one-to-one binding (Hill coefficient $= \sim 0.5$) can be readily interpreted in terms of negative cooperativity between the two bindings sites on the closed and open channel.

The physical picture for $Mg^{2+}$-dependent inactivation that emerges differs fundamentally from one in which a blocker obstructs current flow by lodging within the ion conduction pathway. We speculate that inwardly rectifying $K^+$ channels possesses a gate that is in close proximity to a site that can bind either $Mg^{2+}$ or $K^+$. The gate moves more or less freely at negative membrane potentials between its open and closed positions, but the affinity of the site for $Mg^{2+}$ is high only when it is closed. Accordingly, binding of $Mg^{2+}$ stabilizes the gate in its closed position and the channel does not become free to open until $Mg^{2+}$ dissociates and the site is occupied by $K^+$. A similar model was proposed by Armstrong and Cota (1991) to explain the effects of external $Ca^{2+}$ on the voltage dependence of $Na^+$ channel opening. They suggested that divalent cations stabilize the channel in the closed state by interacting with the

channel voltage sensor. The $Mg^{2+}$-dependent inactivation described here differs in that there is little intrinsic voltage dependence to channel gating.

The mechanism of voltage-dependent gating of inwardly rectifying $K^+$ channels is of interest because the cloning of a channel with similar properties from mouse macrophages shows that it lacks most of the hydrophobic segments characteristic of other voltage-gated $K^+$ channels (Kuno, Baldwin, Jan, and Jan, 1993). Moreover, there is only limited homology of the $NH_2$-terminal region to the S4 region of other voltage-gated $K^+$ channels. The absence of structural elements associated with voltage-dependent gating highlights the importance of the binding of physiological ions in channel gating.

We thank Drs Lily Jan and Julie Schnapf for helpful comments during the course of this work and Michelle LaBotz for help with cell isolations.

Supported by the NIH (J. B. Lansman) and fellowships from the NSF and California Affiliate of the American Heart Association (T. R. Elam).

*Original version recieved 6 January 1994 and accepted version received 3 January 1995.*

## REFERENCES

Armstrong, C. M. 1969. Inactivation of the potassium conductance and related phenomena caused by quaternary ammonium ion injection in squid axons. *Journal of General Physiology.* 54:553–565.

Armstrong, C. M., and G. Cota. 1991. Calcium ion as a cofactor in Na channel gating. *Proceedings National Academy Scienecs, USA.* 88:6528–6531.

Biermans, G., J. Vereecke, and E. Carmeliet. 1987. The mechanism of the inactivation of the inward-rectifying K current during hyperpolarizing steps in guinea-pig ventricular myocytes. *Pflügers Archiv.* 410:604–613.

Blatz, A. I., and K. L. Magleby. 1986. Correcting single channel data for missed events. *Biophysical Journal.* 49:967–980.

Blinks, J. R., W. G. Wier, P. Hess, and F. G. Prendergast. 1982. Measurement of $Ca^{2+}$ concentrations in living cells. *Progress in Biophysics and Molecular Biology.* 40:1–114.

Burton, F. L., and O. F. Hutter. 1989. Properties of 'inwardly rectifying' potassium channels from mammalian sarcolemmal vesicles in absence of "intracellular" $Mg^{2+}$. *Journal of Physiology.* 409:51P. (Abstr.)

Colquhoun, D., and F. J. Sigworth. 1983. Fitting and statistical analysis of single-channel records. In Single Channel Recording. B. Sakmann and E. Neher, editors. Plenum Publishing Corp., New York.

Elam, T. R., and J. B. Lansman. 1990. Voltage-dependent gating of inward-rectifying potassium channels in aortic endothelial Cells. *Biophysics Journal.* 51:A5. (Abstr.)

Elam, T. R., and J. B. Lansman. 1992. Magnesium-dependent gating of inwardly-rectifying potassium channels in aortic endothelial cells. *Biophysics Journal.* 53:A251. (Abstr.)

Fukushima, Y. 1982. Blocking kinetics of the anomalous potassium rectifier of tunicate egg studied by single channel recording. *Journal of Physiology.* 331:311–331.

Hagiwara, S., S. Miyazaki, and N. P. Rosenthal. 1976. Potassium current and the effect of cesium on this current during anomalous rectification of the egg cell membrane of a starfish. *Journal of General Physiology.* 67:621–638.

Hagiwara, S., and K. Takahashi. 1974. The anomalous rectification and cation selectivity of the membrane of a starfish egg cell. *Journal of Membrane Biology.* 18:61–80.

Hamill, O. P., A. Marty, E. Neher, B. Sakmann, and F. J. Sigworth. 1981. Improved patch clamp techniques for high resolution current recordings from cells and cell-free membrane patches. *Pflügers Archiv.* 391:85–100.

Harvey, R. D., and R. E. Ten Eick. 1989. Voltage-dependent block of cardiac inward-rectifying potassium current by monovalent cations. *Journal of General Physiology.* 94:349–361.

Ishihara, K., T. Mitsuiye, A. Noma, and M. Takano. 1989. The $Mg^{2+}$ block and intrinsic gating underlying inward rectification of the $K^+$ current in guinea-pig cardiac myocytes. *Journal of Physiology.* 419:297–320.

Jaffe, E. A., R. L. Nachman, C. G. Becker, and C. R. Minick. 1973. Culture of human endothelial cells derived from umbilical veins. *Journal of Clinical Investigation.* 52:2745–2756.

Johns, A., A. D. Freay, D. J. Adams, T. W. Lategan, U. S. Ryan, and C. VanBreemen. 1988. Role of calcium in the activation of endothelial cells. *Journal of Cardiovascular Pharmacology.* 5:S119–123.

Kubo, Y., T. J. Baldwin, Y. N. Jan, and L. Y. Jan. 1993. Primary structure and functional expression of a mouse inward rectifier potassium channel. *Nature.* 362:127–133.

Kurachi, Y. 1985. Voltage-dependent activation of the inward rectifier potassium channel in the ventricular cell membrane of the guinea pig heart. *Journal of Physiology.* 336:365–385.

Kurachi, Y., T. Nakajima, and T. Sugimoto. 1986. Role of intracellular $Mg^{2+}$ in the activation of muscarinic $K^+$ channel in cardiac atrial cell membrane. *Pflügers Archiv.* 407:572–574

Matsuda, H. 1991. Magnesium gating of the inwardly rectifying $K^+$ channel. *Annual Review of Physiology.* 53:289–298.

Matsuda, H. 1988. Open-state substructure of inwardly rectifying potassium channels revealed by magnesium block of guinea-pig heart cells. *Journal of Physiology.* 397:237–258.

Matsuda, H., A. Saigusa, and H. Irisawa. 1987. Ohmic conductance through the inwardly rectifying K channel and blocking by internal $Mg^{2+}$. *Nature.* 325:156–159.

Matsuda, H., and P. R. Stanfield. 1989. Single inwardly rectifying potassium channels in cultures muscle cells from rat and mouse. *Journal of Physiology.* 414:111–124.

McKinney, L. C., and E. K. Gallin. 1988. Inwardly rectifying whole-cell and single-channel K currents in the murine macrophage cell line J774.1. *Journal of Membrane Biology.* 103:41–53.

Ogden, D. C., and D. Colquhoun. 1985. Ion channel block by acetylcholine, carbachol and suberyldicholine at the frog neuromuscular junction. *Proceedings of the Royal Society B.* 225:329–355.

Ohmori, H. 1978. Inactivation kinetics and steady-state current noise in the anomalous rectifier of tunicate egg cell membrane. *Journal of Membrane Biology.* 53:143–156.

Ohmori, H., and M. Yoshii. 1977. Surface potential reflected in both gating and permeation mechanisms of sodium and calcium channels of the tunicate cell membrane. *Journal of Physiology.* 267:429–463.

Olesen, S.-P., D. E. Clapham, and P. F. Davies. 1988. Haemodynamic shear stress activates a $K^+$ current in vascular endothial cells. *Nature.* 331:168–331.

Pearson, J. D., L. L. Slakey, and J. L. Gordon. 1983. Stimulation of prostaglandin production through purinoceptors on cultured porcine endothelial cells. *Biochemical Journal.* 214:273–276

Sakmann, B., and G. Trube. 1984*a*. Conductance properties of single inwardly-rectifying potassium channels in ventricular cells from guinea-pig heart. *Journal of Physiology.* 347:641–657.

Sakmann, B., and G. Trube. 1984*b*. Voltage-dependent inactivation of inward-rectifying single-channel currents in the guinea-pig heart cell membrane. *Journal of Physiology.* 347:659–683.

Shioya, T., H. Matsuda, and A. Noma. 1993. Fast and slow blockades of the inward-rectifier K+ channel by external divalent cations in guinea-pig cardiac myocytes. *Pflügers Archiv.* 422:427–435.

Silver, M. R., and T. E. DeCoursey. 1990. Intrinsic gating of inward rectification bovine pulmonary artery endothelial cells in the presence or absence of internal $Mg^{2+}$. *Journal of General Physiology.* 96:109–133.

Standen, N. B., and P. R. Stanfield. 1980. Rubidium block and rubidium permeability of the inward rectifier of frog skeletal muscle fibers. *Journal of Physiology.* 304:415–435.

Takeda, K., V. Schini, and H. Stoeckel. 1987. Voltage-activated potassium, but not calcium currents in cultured bovine aortic endothelial cells. *Pflügers Archiv.* 410:385–393.

Vandenberg, C. A. 1987. Inward rectification of a potassium channel in cardiac ventricular cells depends on internal magnesium ions. *Proceedings of the National Academy of Sciences, USA.* 85:2560–2564.

Woodhull, A. 1973. Ionic blockage of sodium current in nerve. *Journal of General Physiology.* 61:687–708